IEEE Photonics Journal
An IEEE Photonics Society Publication

An Optical Fiber Tip Micrograting Thermometer

Volume 3, Number 5, October 2011

Jing Feng
Ming Ding
Jun-Long Kou
Fei Xu
Yan-Qing Lu

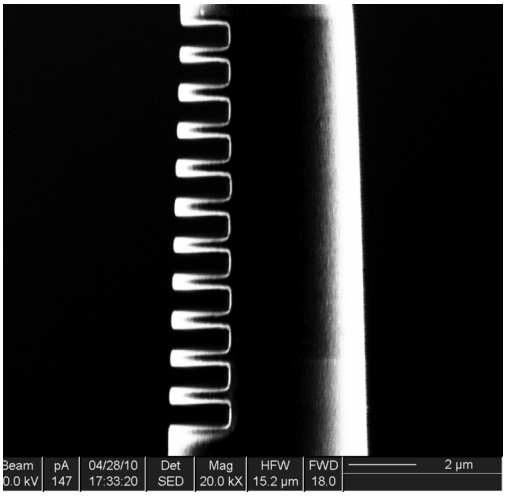

DOI: 10.1109/JPHOT.2011.2165835
1943-0655/$26.00 ©2011 IEEE

An Optical Fiber Tip Micrograting Thermometer

Jing Feng,[1] Ming Ding,[2] Jun-Long Kou,[1] Fei Xu,[1] and Yan-Qing Lu[1]

[1]College of Engineering and Applied Sciences and National Laboratory of Solid State Microstructures, Nanjing University, Nanjing 210093, China
[2]Optoelectronics Research Centre, SO17 1BJ Southampton, U.K.

DOI: 10.1109/JPHOT.2011.2165835
1943-0655/$26.00 ©2011 IEEE

Manuscript received July 3, 2011; accepted August 10, 2011. Date of publication August 22, 2011; date of current version September 13, 2011. This work was supported by the National 973 program under Contract 2010CB327800 and Contract 2011CBA00205 and the National Science Foundation of China under program 11074117 and program 60977039. Corresponding author: F. Xu (e-mail: feixu@nju.edu.cn).

Abstract: An ~12-μm-long Bragg grating was engraved in an ~5-μm-diameter optical fiber tip by focused ion beam (FIB) milling. An ~10-dB extinction was achieved at 1570 nm with only 11 indentations. The grating was used for temperature sensing, and it exhibited a temperature sensitivity of ~22 pm/°C.

Index Terms: Fiber gratings, optical fiber devices, optical fiber sensors, temperature sensors.

Since their discovery in 1978 [1], optical fiber gratings have found a variety of applications in telecom and sensing because of their relatively low cost, inherent self-referencing, and multiplexing/demultiplexing capabilities. Over the last two decades, fiber Bragg gratings (FBGs) have been manufactured mainly by modifying the core refractive index using interferometric or point-by-point techniques; most of interferometric techniques use a phase mask and an ultraviolet (UV) laser [2] (typically excimer or frequency doubled Ar^+ ion) or femtosecond lasers (near infrared [3] or UV [4]). Gratings based on surface etched corrugations have also been demonstrated in etched fibers using photolithographic techniques [5]. However, all these gratings fabricated in thick fibers have weak refractive index modulations ($\Delta n_{\mathrm{mod}} \sim 10^{-4}$–$10^{-3}$), and the related grating lengths are on the order of several millimeters. To reduce the grating length, strong refractive index modulations ($\Delta n_{\mathrm{mod}} > 10^{-1}$) are necessary. Strong Δn_{mod} can be obtained alternating layers of different materials, one of which can be air. Although this process in normal optical fibers imposes the removal of large amounts of material (the propagating mode is confined at a depth > 50 μm from the fiber surface), in fiber tapers and tips, it requires the removal of small amounts of matter because the propagating mode is confined be the silica/air interface. Few techniques have been proposed for the fabrication of gratings in microfibers, including photorefractive inscription using CO_2 lasers [6], femtosecond lasers [7], [8], and wrapping a microfiber on a microstructured rod [9]. None of them produced strong and short Bragg gratings. In some cases, extra polymer coatings are needed, while in others, the use of CO_2 lasers implies that the grating length is still long (it only can be used to write long period gratings (LPGs) or high-order FBG). As a consequence, devices based on gratings tend to have a sizeable length. Typically, FBGs have lengths in the order of few millimeters; thus, thermometers exploiting FBGs have lengths well in excess of 1 mm.

In this paper, an ultrasmall FBG is machined into a nonphotosensitive fiber tip by focused ion beam (FIB) milling. FIB milling is highly suitable for nanofabrication due to its small and controllable

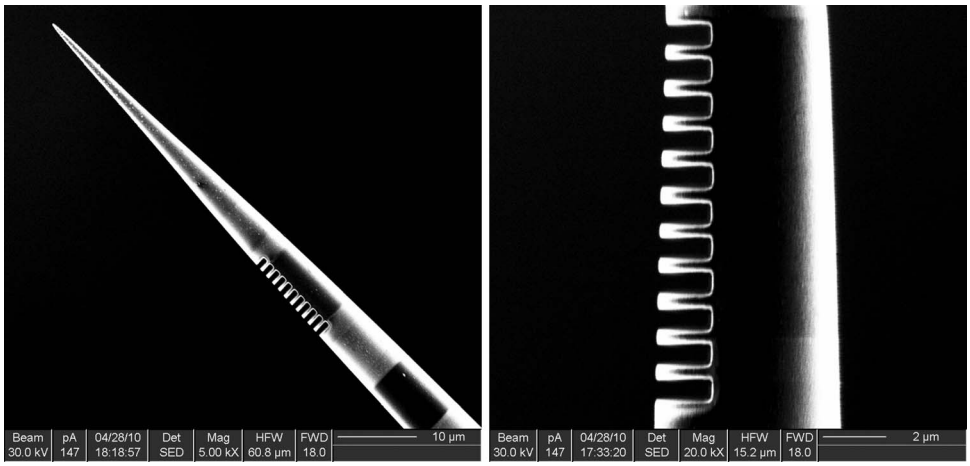

Fig. 1. (Left) SEM picture of the nanostructured MFT. The grating has 11 notches and a total length of $\sim$12 μm. The notch length and depth are $\sim$0.6 μm and $\sim$1.6 μm, respectively. The grating period is $\Lambda \sim 1.1$ μm. (Right) Magnified image of the grating region.

spot size, and it has been previously used to fabricate Fabry–Perot microcavities [10], [11] and a plasmonic device [12]–[15] in optical fiber tips. Here, grooves are periodically carved on a sharp microfiber tip (MFT) with an $\sim$5-μm diameter.

The MFT was fabricated using a commercial pipette puller (Sutter Inc., Novato, USA) [12], [15]. The tip was coated with a thin layer of aluminum (to avoid charging during machining), fixed to a metallic substrate using conductive tape, and then placed in the FIB chamber (Strata FIB 201, FEI Inc., Hillsboro, USA) perpendicularly to the gallium ion beam. The beam diameter was $\sim$30 nm, providing a suitable accuracy to precisely control the groove size. The grating was made through two identical processing steps: the second FIB milling was used to improve surface smoothness. The nanostructured fiber tip was then immersed in hydrochloric acid for about 20 min to completely remove the aluminum layer and then cleaned with deionized water.

Fig. 1 shows an SEM micrograph of the nanostructured MFT. The grating has 11 shallow corrugations with period $\Lambda = 1.1$ μm, providing a total length of $\sim$12 μm, which is two orders of magnitude shorter than FBGs fabricated in conventional optical fiber. Each notch is $\sim$1.6 μm deep and $\sim$0.6 μm long. The tip average radius at the position where the notches are located is $r \sim 2.7$ μm. The Bragg wavelength of the grating can be calculated from $\lambda_B = 2n_{eff}\ /\mathrm{m}$, where n_{eff} is the mode effective refractive index in the equivalent unperturbed geometry, Λ is the period, and m is the Bragg order. Unlike conventional circularly symmetric FBGs, this nanostructured MFT has asymmetric periodic corrugations. The mode field and n_{eff} in the nanostructured MFT can be derived analytically from the bare MFT using the method developed by Streifer [16], [17], which considers an equivalent structure, which is obtained by shifting the boundary between air and silica to compensate for the different geometry. Using averaged values $r = 2.7$ μm, $\tau = 0.33$, and $h_g = 1.6$ μm, we have the effective index $n_{eff} = 1.428$. The calculated central Bragg wavelength is 1571 nm.

Simulations were carried out using 3-D Finite Element Method (FEM) to numerically solve Maxwell equations in the frequency domain and get the reflectivity of the microfiber tip grating (MFTG). The numerical model was defined, solved, and analyzed using COMSOL 4.1 multiphysics. Both cases of uniform diameter and conical profile were considered. The modeling geometry is presented in Fig. 2(a) and (b). While Fig. 2(b) has the same geometry shown in the SEM micrograph of Fig. 1, Fig. 2(a) has a uniform diameter corresponding to the average diameter. In order to decrease calculation complexity and time, symmetry was used to reduce the geometry to a semi-cylinder. The chosen boundary conditions were perfect electric conductor at the symmetry plane, scattering boundary condition at the cylinder outer surfaces, and port boundary at the input and output surfaces. Simulations were run with controlled mesh size (300 nm in silica, 300 nm in surrounding air, and 150 nm in the notches) to make efficient use of computer memory. A single

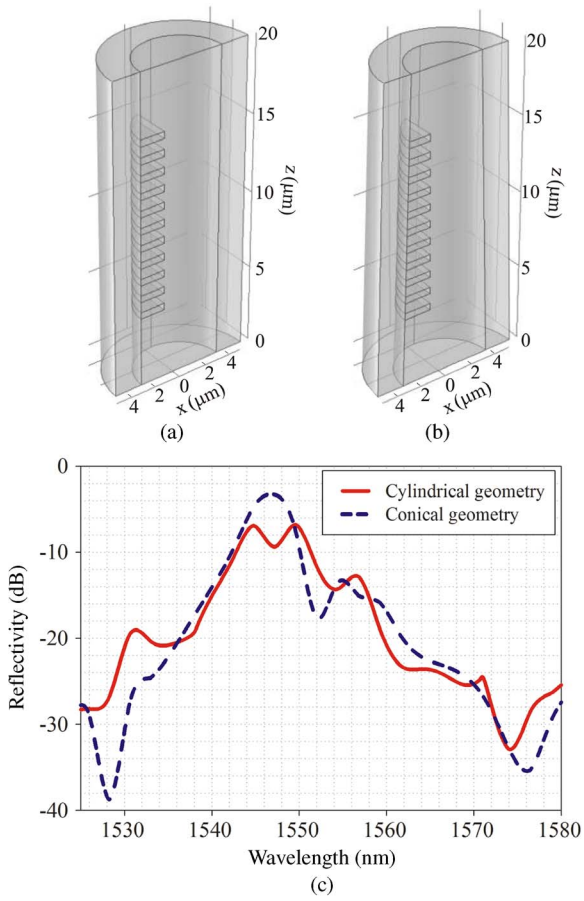

Fig. 2. Modeling geometry of (a) cylindrical and (b) conical profile. (c) Calculated reflectivity for the cylindrical (red solid line) and conical geometry (blue dashed line).

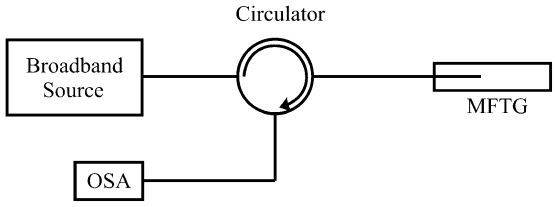

Fig. 3. Experimental setup of characterizing MFTG.

mode was launched into the MFT from the input port. Fig. 2(c) shows the calculated reflectivity for the cylindrical and conical geometries: Both geometries present a peak at $\lambda_B \sim 1547$ nm and with $\sim$30 dB amplitude.

Experimentally, the MFTG of Fig. 1 was characterized with the setup shown in Fig. 3: Light from a broadband source was injected into the MFTG, and the reflected light was then collected by an optical spectrum analyzer (OSA) (Ando AQ6317B, Japan) after passing through a circulator. To test the setup, the MFT reflection was analyzed before grating inscription and displayed a negligible reflection over the whole spectrum: The reflection at the tip end was negligible.

The MFTG thermal response was characterized by placing the sample in a microfurnace and increasing the temperature from room temperature (20 °C) to 230 °C. The microfurnace temperature was measured *in situ* with a thermocouple (TES-1310, Type K, TES Electrical Electronic Corp). The spectrum and temperature were recorded several minutes after the temperature was

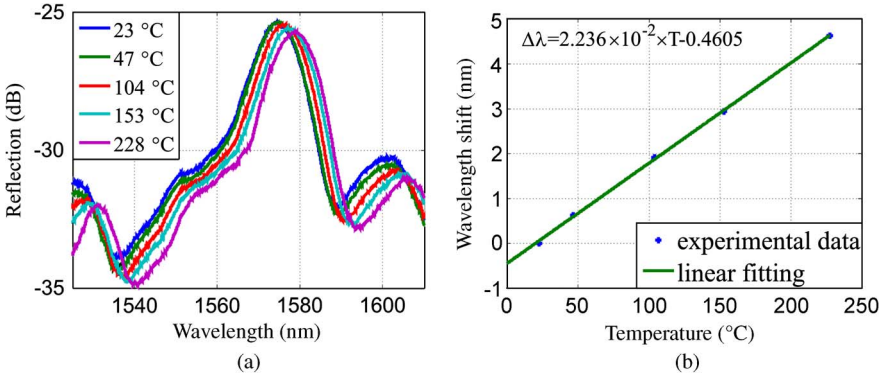

Fig. 4. (a) Reflection spectra of the MFTG in air at different temperatures. (b) Dependence of the measured wavelength shift on temperature. The asterisk represents the measured results while the solid line is the linear fitting result.

changed to avoid unwanted temperature fluctuations and/or spurious effects. The MFTG spectra at different temperatures (23 °C, 47 °C, 104 °C, 153 °C, and 228 °C) are shown in Fig. 4(a). There is a clear peak at ~1572 nm with an extinction of 10 dB at room temperature. Two sidelobes are observed at longer (1600 nm) and shorter (1535 nm) wavelengths. As expected, the spectrum shifts to longer wavelengths when the environment temperature is raised. The possible explanation of the difference between experiment reflection spectrum and simulation spectrum can be the effective indices variation, unperfected notch surfaces, and unperfected grating periodicity.

The temperature sensitivity S is defined as the resonance wavelength shift divided by the corresponding temperature change. S depends on temperature through the thermal expansion and/or thermooptics effect [18]

$$S = \frac{d\lambda_B}{dT} = \frac{2}{m}\left(\Lambda\alpha_T n_{eff} + r\Lambda\alpha_T \frac{\partial n_{eff}}{\partial r} + \sigma_T \Lambda \frac{\partial n_{eff}}{\partial n_{\text{silica}}}\right) \quad (1)$$

where $\sigma_T(1.4 \times 10^{-5}/^{\circ}\text{C})$ is the thermooptic coefficient, and $\alpha_T(5.5 \times 10^{-7}/^{\circ}\text{C})$ is the thermal expansion coefficient. Temperature change influences three aspects: temperature-induced grating length variation, temperature-induced index variation, and taper volume variation. From calculations, it appears that thermal expansion effect [the first and second part of (1)] contributes little to the total sensitivity (< 6%), mainly due to the low thermal expansion coefficient of silica. The third contribution is about $15 \sim 20$ pm/°C and dominates in temperature sensing. Moreover, $\partial n_{eff}/\partial n_{\text{silica}} \sim 1$ means that the most efficient method to increase thermal sensitivity is to use fibers with high σ_T.

Fig. 4(b) displays the measured Bragg wavelength shift $(\Delta\lambda)$ on the temperature (T). A linear fit with slope $S \sim 22$ pm/°C is used across the entire calibration range. The average sensitivity S is very close to the theoretical result, and it is higher than or similar with previous fiber grating sensors.

In conclusion, we experimentally demonstrate an extremely short all-silica FBG by nanostructuring an MFT with FIB milling. COMSOL simulations were carried out to verify the strong reflection of MFTG. The 12-μm-long grating was used for temperature sensing and exhibited a linear sensitivity of S ~ 22 pm/°C. Its advantages of ultracompact size, high sensitivity, easy interrogation, simple fabrication, and unique geometry offer great prospects for high-resolution temperature mapping and temperature sensors for ultrasmall spaces and large temperature gradients.

Acknowledgment

The authors also acknowledge the support from the New Century Excellent Talents program and the Changjiang scholars program.

References

[1] K. O. Hill, Y. Fujii, D. C. Johnson, and B. S. Kawasaki, "Photosensitivity in optical fiber waveguides: Application to reflection filter fabrication," *Appl. Phys. Lett.*, vol. 32, no. 10, pp. 647–649, May 1978.

[2] K. O. Hill, B. Malo, F. Bilodeau, D. C. Johnson, and J. Albert, "Bragg gratings fabricated in monomode photosensitive optical fiber by UV exposure through a phase mask," *Appl. Phys. Lett.*, vol. 62, no. 10, pp. 1035–1037, Mar. 1993.

[3] S. J. Mihailov, C. W. Smelser, P. Lu, R. B. Walker, D. Grobnic, H. Ding, G. Henderson, and J. Unruh, "Fiber Bragg gratings made with a phase mask and 800-nm femtosecond radiation," *Opt. Lett.*, vol. 28, no. 12, pp. 995–997, Jun. 2003.

[4] S. A. Slattery, D. N. Nikogosyan, and G. Brambilla, "Fiber Bragg grating inscription by high-intensity femtosecond UV laser light: Comparison with other existing methods of fabrication," *J. Opt. Soc. Amer. B*, vol. 22, no. 2, pp. 354–361, Feb. 2005.

[5] C. Y. Lin and L. A. Wang, "A wavelength- and loss-tunable band-rejection filter based on corrugated long-period fiber grating," *IEEE Photon. Technol. Lett.*, vol. 13, no. 4, pp. 332–334, Apr. 2001.

[6] H. Xuan, W. Jin, and M. Zhang, "CO_2 laser induced long period gratings in optical microfibers," *Opt. Exp.*, vol. 17, no. 24, pp. 21 882–21 890, Nov. 2009.

[7] H. Xuan, W. Jin, and S. Liu, "Long-period gratings in wavelength-scale microfibers," *Opt. Lett.*, vol. 35, no. 1, pp. 85–87, Jan. 2010.

[8] A. Martinez, I. Y. Khrushchev, and I. Bennion, "Thermal properties of fibre Bragg gratings inscribed point-by-point by infrared femtosecond laser," *Electron. Lett.*, vol. 41, no. 4, pp. 176–178, Feb. 2005.

[9] F. Xu, G. Brambilla, J. Feng, and Y.-Q. Lu, "A microfiber Bragg grating based on a microstructured rod: A proposal," *IEEE Photon. Technol. Lett.*, vol. 22, no. 4, pp. 218–220, Feb. 2010.

[10] J.-l. Kou, J. Feng, Q.-J. Wang, F. Xu, and Y.-Q. Lu, "Microfiber-probe-based ultrasmall interferometric sensor," *Opt. Lett.*, vol. 35, no. 13, pp. 2308–2310, Jul. 2010.

[11] J.-l. Kou, J. Feng, L. Ye, F. Xu, and Y.-Q. Lu, "Miniaturized fiber taper reflective interferometer for high temperature measurement," *Opt. Exp.*, vol. 18, no. 13, pp. 14 245–14 250, Jun. 2010.

[12] F. Renna, D. Cox, and G. Brambilla, "Efficient sub-wavelength light confinement using surface plasmon polaritons in tapered fibers," *Opt. Exp.*, vol. 17, no. 9, pp. 7658–7663, Apr. 2009.

[13] G. Brambilla, "Optical fibre nanotaper sensors," *Opt. Fiber Technol.*, vol. 16, no. 6, pp. 331–342, Dec. 2010.

[14] G. Brambilla, "Optical fibre nanowires and microwires: A review," *J. Opt.*, vol. 12, no. 4, p. 043001, Apr. 2010.

[15] G. Brambilla, F. Xu, P. Horak, Y. Jung, F. Koizumi, N. P. Sessions, E. Koukharenko, X. Feng, G. S. Murugan, J. S. Wilkinson, and D. J. Richardson, "Optical fiber nanowires and microwires: Fabrication and applications," *Adv. Opt. Photon.*, vol. 1, no. 1, pp. 107–161, Jan. 2009.

[16] W. Streifer, D. Scifres, and R. Burnham, "Coupling coefficients for distributed feedback single- and double-heterostructure diode lasers," *IEEE J. Quantum Electron.*, vol. QE-11, no. 11, pp. 867–873, Nov. 1975.

[17] W. Streifer and A. Hardy, "Analysis of two-dimensional waveguides with misaligned or curved gratings," *IEEE J. Quantum Electron.*, vol. QE-14, no. 12, pp. 935–943, Dec. 1978.

[18] H. Y. Choi, K. S. Park, S. J. Park, U. C. Paek, B. H. Lee, and E. S. Choi, "Miniature fiber-optic high temperature sensor based on a hybrid structured Fabry–Perot interferometer," *Opt. Lett.*, vol. 33, no. 21, pp. 2455–2457, Nov. 2008.